Research Paper

Silencing of circCYP51A1 represses cell progression and glycolysis by regulating miR-490-3p/KLF12 axis in osteosarcoma under hypoxia

Jian Yang [*], Zhiwei Liu, Ben Liu, Lishan Sun

Four Department of Orthopaedics, Cangzhou Central Hospital, China

HIGHLIGHTS

- CircCYP51A1 was up-regulated in osteosarcoma cells under hypoxia.
- CircCYP51A1 mediated KLF12 expression through sponging miR-490-3p.
- Under hypoxia condition, circCYP51A1 knockdown inhibited cell progression and glycolysis by regulating miR-490-3p/ KLF12 axis.

ARTICLE INFO

ABSTRACT

Background: Hypoxia is a key characteristic of osteosarcoma (OS). Increasing data suggested that circular RNA (circRNAs) were involve in the progression of cancers and the regulation of hypoxia, including OS. This study aims to examine the biological mechanism of circRNA cytochrome P450 family 51 subfamily A member 1 (circCYP51A1) in OS under hypoxia.

Methods: The expression levels of circCYP51A1, microRNA-490-3p (miR-490-3p) and kruppel-like factor 12 (KLF12) were detected by quantitative real-time polymerase chain reaction (qRT-PCR) in OS tissues and cells. Cell proliferation, migration and invasion were determined by colony formation assay and transwell assay. Lactate production and glucose consumption in OS cells were measured by using lactate assay kit and glucose assay kit, respectively. Western blot assay and immunohistochemistry assay were used to test protein levels. The associated relationship between miR-490-3p and circCYP51A1 or KLF12 was predicted using Starbase or DIANA online database and verified by dual-luciferase reporter assay. The xenograft model was used to explore the role of circCYP51A1 *in vivo*.

Results: CircCYP51A1 and KLF12 expression were dramatically increased, whereas miR-490-3p was decreased in OS cells under hypoxia condition. Deficiency of circCYP51A1 hindered hypoxia-induced cell proliferation, migration, invasion and glycolysis in OS cells. CircCYP51A1 enhanced KLF12 expression by sponging miR-490-3p. MiR-490-3p inhibitor weakened the inhibition effect of circCYP51A1 knockdown on the progression of OS under hypoxia. Besides, overexpression of miR-490-3p inhibited cell progression of OS under hypoxia condition, while the effects were attenuated by KLF12 overexpression. Importantly, knockdown of circCYP51A1 inhibited tumor growth *in vivo*.

Conclusion: CircCYP51A1 mediated cell proliferation, migration, invasion and glycolysis by regulating miR-490-3p/KLF12 axis in OS cells under hypoxia condition.

1. Introduction

As a primary malignant tumor, osteosarcoma (OS) is one of the causes of death in children and adolescents [1]. It most often occurs in bones and is highly aggressive [2]. Although some results have been achieved in radiotherapy and chemotherapy, the prognosis of OS patients is still very poor [3]. Hypoxia is an important characteristic of solid tumor microenvironment, which is caused by rapid tumor growth and relatively low density of microvessels [4]. Studies have shown that hypoxia can participate in the proliferation, metastasis, glycolysis and angiogenesis of cancer patients [5–7]. Therefore, it is urgent to explore the progress and pathogenesis of OS under hypoxia.

CircRNAs (circular RNAs) are a special type of single-stranded ncRNAs (non-coding RNAs) with a closed continuous circular structure (without 5′cap or 3′polyA tail), and are more stable than linear RNAs [8]. Increasing evidence shows that circRNAs play significant roles in the carcinogenesis of various kinds of tumors, including OS [9]. CircUBE2D2 deficiency impeded breast cancer (BC) cell proliferation, metastasis and doxorubicin resistance but boosted cell apoptosis by sponging miR-512-3p/CDCA3 axis [10]. Up-regulation of circ_0042823 promoted cancer progression of laryngeal squamous cell carcinoma (LSCC) [11]. Furthermore, circRNAs participate in the occurrence and development of tumors in hypoxia condition. Knockdown of circ-SLAMF6 suppressed gastric cancer (GC) cell glycolysis and metastasis by regulating miR-204-5p and MYH9 under hypoxia [12]. Silencing of circ_0001982 inhibited BC cell progression by up-regulating miR-1287-5p and down-regulating MUC19 under hypoxia [13]. Hsa_circ_0081001 (circCYP51A1), originating from cytochrome P450 family 51 subfamily A member 1, is located at chromosome 7: 91755566–91756945 with a length of 302 bp. The expression level of hsa_circ_0081001 was increased in OS tissues than in adjacent non-tumor tissues in previous work [14]. Nevertheless, the molecular mechanism and biological function of circCYP51A1 in the progression of OS under hypoxia remain largely unknown.

Recent research indicated that circRNAs, as endogenous RNAs, regulated gene expression by specific sponging microRNAs (miRNAs) [15]. miRNAs (22 nucleotides), a class of small non-coding RNA molecules, primarily regulate gene expression by binding to the 3′UTR (untranslated region) of mRNAs [16,17]. A large number of miRNAs are maladjusted in diverse human tumors and play an important role in many malignant behaviors as carcinogenic or tumor suppressor factors [18]. Previous works have exhibited that miR-490-3p is a tumor - repressor in human diseases, such as prostate cancer (PCa) [19], non-small cell lung cancer (NSCLC) [20] and gastric cancer (GC) [21]. Furthermore, miR-490-3p has been reported to be expressed at a low level in OS tissues [22]. Nevertheless, the molecular mechanism of miR-490-3p in OS under hypoxic condition has not been discussed.

KLF12 (Kruppel-like factor 12), is a member of the KLF family, plays a pivotal role in several human cancers, such as hepatocellular carcinoma (HCC) [23], nasopharyngeal carcinoma (NPC) [24] and GC [25]. Additionally, the expression level of KLF12 in OS tissues was strikingly boosted [26]. Yet, the mechanism of KLF12 requires further exploration in OS under hypoxia environment.

The purpose of this research is to appraise the functions of circ-CYP51A1 on OS cell proliferation, migration, invasion and glycolysis under hypoxia condition. Moreover, this study explored the biological mechanism of circCYP51A1/miR-490-3p/KLF12 axis in OS cells under hypoxia. Our information may offer a new therapeutic target for efficient therapy of OS.

2. Materials and methods

2.1. Tissue samples

Thirty-three pairs of OS tissues and neighboring normal samples were obtained from OS patients, who underwent surgery at Cangzhou Central Hospital. None of OS patients accepted any preoperative treatment. The resected fresh samples were promptly transferred into liquid nitrogen and then conserved at −80 °C. Prior to this research, written informed consent was obtained from each participant, and this research was authorized by the institutional ethics committee of Cangzhou Central Hospital.

2.2. Cell culture, hypoxia treatment and transfection

Human osteoblast cell line (hFOB1.19) and OS cell lines (U2OS and MG63) were commercially obtained from American Type Culture Collection (ATCC, Manassas, VA, USA) and maintained in RPMI–1640 medium including 10 % fetal bovine serums (FBS, Gibco, Grand Island, NY, USA) and 100 U/mL penicillin/streptomycin (Biochrom, Berlin, Germany) in a humidified incubator with 5 % CO_2 at 37 °C. To establish the hypoxic condition, U2OS and MG63 cells were placed in an incubator with oxygen O_2 (1 %), CO_2 (5 %) and N_2 (94 %) for 0 h, 3 h, 6 h, 12 h, 24 h, and 48 h.

The small interfering RNAs (siRNAs) against circCYP51A1 (si-circ-CYP51A1) and KLF12 (si-KLF12), non-targeted siRNA (si-NC), miR-490-3p mimic (miR-490-3p), mimic negative control (miR-NC), miR-490-3p inhibitors (in-miR-490-3p) and inhibitor negative control (in-miR-NC) were obtained by GenePharma (Shanghai, China). KLF12 over-expression vector (KLF12) was synthesized by inserting the homologous sequence of KLF12 into pcDNA3.1 (Thermo Fisher), and pcDNA3.1 -vector (pcDNA) was used as a negative control. OS (U2OS and MG63) cells were transfected with the above oligonucleotides or plasmids using Lipofectamine 3000 (Thermo Fisher Scientific).

2.3. Quantitative real-time polymerase chain reaction (qRT-PCR)

Based on the manufacturer's directions, the total RNA of OS tissues and cells was extracted by using Trizol kit (Thermo Fisher Scientific Inc., Waltham, MA, USA). cDNA reverse transcription kit (Thermo Fisher Scientific Inc.,) was used to reverse total RNA into cDNA and then SYBR Premix Ex Taq kit (Thermo Fisher Scientific Inc.,) was used to conduct qRT-PCR analysis. The response conditions were shown as below: predenaturation was carried out at 95 °C for 2 min, then 40 cycles were performed at 95 °C for 10 s, 60 °C for 20 s, and finally extended at 72 °C for 7 min. The $2^{-\Delta\Delta Ct}$ method was used to analyze the relative RNA expression levels of circCYP51A1, miR-490-3p and KLF12. Small nuclear RNA U6 and beta-actin (β-actin) were exploited as endogenous controls. All primer sequences are presented as below: circCYP51A1 forward 5′-TGCCTAGTTTCAGGTTTTCTTGG-3′ circCYP51A1 reverse 5′-CCACTTTCTCCCCAACTCTCA-3′, miR-490-3p forward 5′-GCCGAG-CAACCTGGAGGACTCC-3′; miR-490-3p reverse 5′-CTCAACTGGTGTCGTGGAG-3′; KLF12 forward 5′-GTCAATAAA-CAAAGCCAGGAC-3′ and KLF12 reverse 5′-ACGAAGATGACGCTGAA-GATA-3′.

2.4. RNase R treatment and subcellular localization analysis

To verify the characteristics of circRNA, total RNAs (2.5 μg/groups) were isolated from U2OS and MG63 cells and cultured with 10 U RNase R (Qiagen, Valencia, CA, USA) for 30 min at 37C. The abundance of circCYP51A1 and GAPDH mRNA was detected by using qRT-PCR.

PARIS isolation kit (Thermo Fisher Scientific) was used for the detection of circCYP51A1 cellular localization. U2OS and MG63 cells were collected and cultured in 200 μL Lysis Buffer on ice. After centrifugation, the supernatant including cytoplasmic RNA was gathered and the remaining fraction contained nuclear RNA. CircCYP51A1 expression level was analyzed by qRT-PCR.

2.5. Colony formation assay

U2OS and MG63 cells with transfections were seeded in 6-well plates (500 cells per well) at 37 °C for two weeks. Subsequently, cells were washed by using phosphate-buffered saline (PBS) and fixed with paraformaldehyde (4 %) (Beyotime, China). The colonies were stained with crystal violet (0.5 %) for 30 min at normal atmospheric temperature. Photographs were obtained and the cell numbers were manually counted.

2.6. Transwell assay

The 24-well Transwell chambers (Corning, Shanghai, China) were utilized to explore the migratory capacities of U2OS and MG63 cells. The transfected cells (200 μL, 5×10^4 cells/well) were placed in the upper
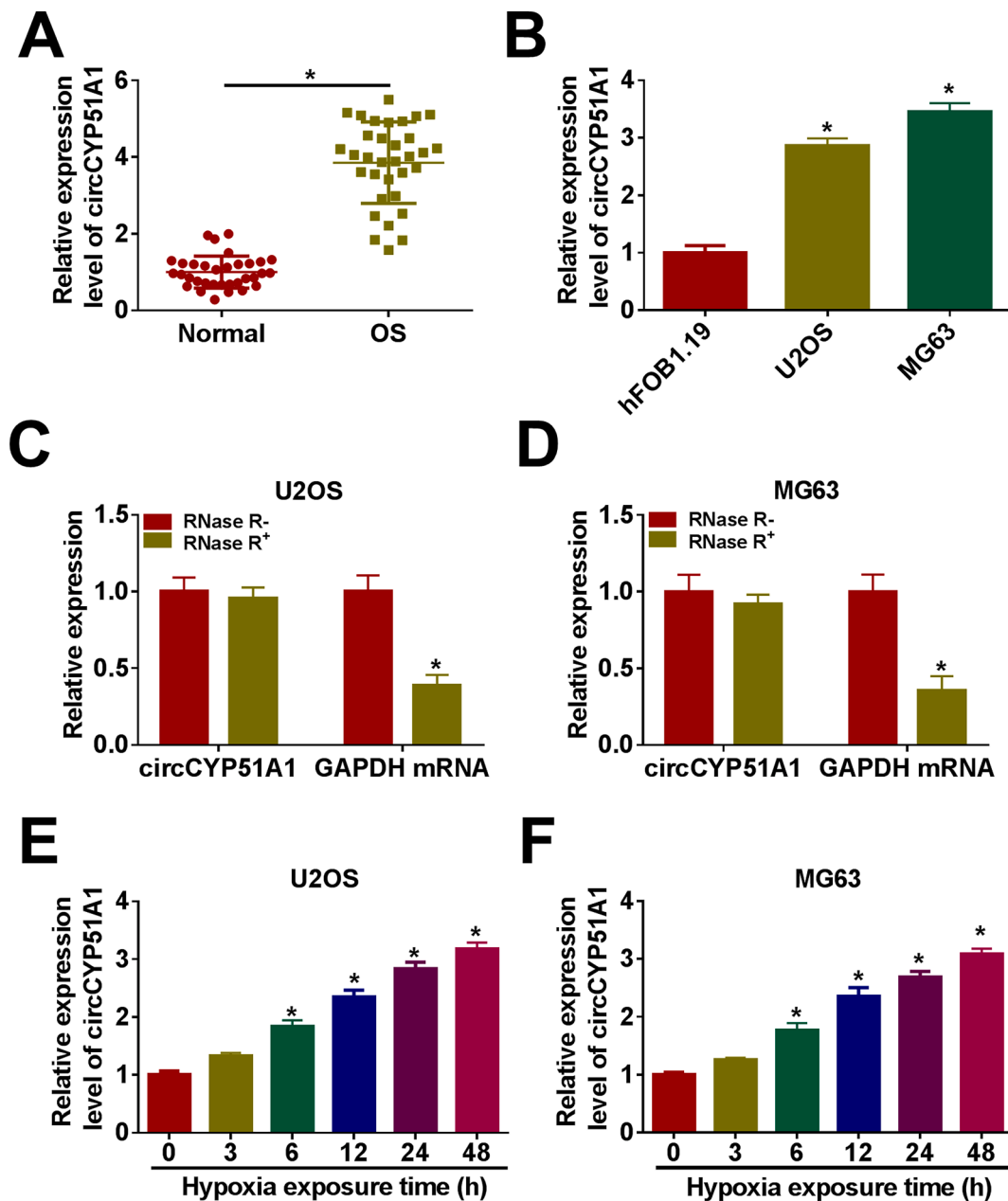
Fig. 1. The abundance of circCYP51A1 was up-regulated in OS cells under hypoxia. (A) The expression of circCYP51A1 was determined by qRT-PCR in OS tissues (n = 33) and neighboring normal samples (n = 33). (B) CircCYP51A1 expression in OS cell lines (U2OS and MG63) and human osteoblast cell line (hFOB1.19) was examined by qRT-PCR. (C-D) The expression level of circCYP51A1 was determined in U2OS and MG63 cells with or without RNase R treatment. (E-F) Relative expression of circCYP51A1 in U2OS and MG63 cells exposed to hypoxia treatment for 0, 3, 6, 12, 24, or 48 h was detected by qRT-PCR. *$P < 0.05$.

chambers, and the lower chambers were filled with 600 μL RPMI-1640 medium comprising 10 % FBS. After 24 h of incubation in hypoxic or normoxic conditions, the cells that invaded or migrated through the membranes were fixed with paraformaldehyde (4 %) and dyed with crystal violet (0.1 %). The cells were then photographed and counted by a microscope (Nikon, Tokyo, Japan). The diluted Matrigel was pre-coated in the upper chambers in the invasion assay and other steps were alike to the migration experiment.

2.7. Wound healing assay

Under hypoxic or normoxic condition, 5×10^5 cells/mL U2OS and MG63 cells were cultured in RPMI-1640 medium containing 10 % FBS and 100 U/mL penicillin–streptomycin until the cell confluence reached around 100 %. Single-line scratches were generated by using a sterile

pipette tip. The cells were washed and the wound surface was photo-graphed at 0 h and 24 h by using a microscope (magnification, ×100).

2.8. Lactate production and glucose consumption

U2OS and MG63 cells (1×10^5 /well) were plated onto 12-well plates overnight and exposed to hypoxia treatment for 48 h, with nor-moxia group (or si-NC or miR-NC) used as a control. Afterwards, lactic acid Assay kit (Solarbio, Beijing, China) and glucose Assay kit (Solarbio) were utilized to determine lactic acid production and glucose con-sumption, respectively.

2.9. Western blot (WB) assay

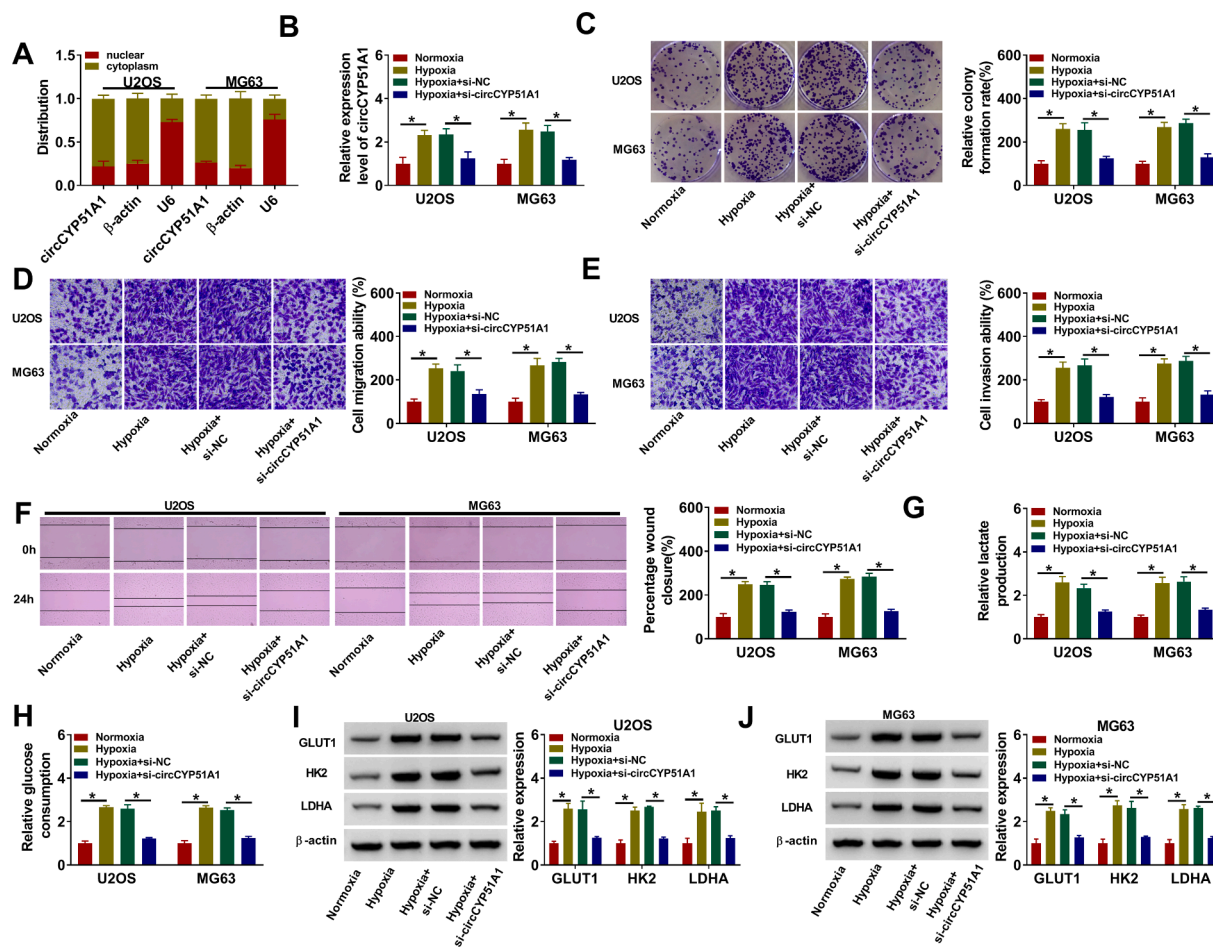Total protein of OS cells and tissues were separated using lysis buffer

Fig. 2. Silencing of circCYP51A1 impeded the proliferation, migration, invasion and glycolysis of OS cells under hypoxia. (A) Subcellular distribution of circ-CYP51A1 was analyzed by qRT-PCR in U2OS and MG63 cells. U2OS and MG63 cells were transfected with si-NC or si-circCYP51A1 after hypoxia treatment for 48 h. (B) CircCYP51A1 expression was measured by qRT-PCR. (C) Colony formation assay was used to analyze cell proliferation. (D-E) Transwell assays were performed to determine migration and invasion. (F) Wound healing assay was used to detect cell migration. (G-H) Lactate production and glucose consumption levels in U2OS and MG63 cells were detected using lactate and glucose assay kits, respectively. (G) The levels of glycolysis-related proteins (GLUT1, HK2 and LDHA) were examined by western blot. *$P < 0.05$.

including RIPA (radioimmunoprecipitation assay, Beyotime, Shanghai, China). The protein samples were centrifuged in a 4 °C centrifugation for 20 min at 13,000 g and the supernatant was harvested and boiled. Subsequently, sodium dodecyl sulfate polyacrylamide gel electrophoresis (SDS-PAGE) was used to separate the protein sample (25 mg). The protein samples were transferred onto the PVDF (polyvinydene fluoride, Millipore, Billerica, MA, USA) membrane. Next, the PVDF membranes were probed with the appropriate primary antibodies purchased from Abcam, including anti-Glucose Transporter GLUT1 antibody (anti-GLUT1; 1:1000, ab115730), anti-Hexokinase II (anti-HK2; 1:1000, ab273721), anti-Lactate Dehydrogenase (anti-LDHA; 1:8000, ab52488), anti-KLF12 (1:1000, ab129459), and anti-beta-actin (anti-β-actin; 1:1000, ab8226) at 4 °C for overnight. The membranes were washed and cultured with secondary antibodies (IgG H&L, ab205718, Abcam). BeyoECL Plus (Beyotime) was used to visualize the protein bands and β-actin was utilized as an internal control.

2.10. Dual-luciferase reporter assay

The binding sites between miR-490-3p and circCYP51A1 or KLF12 were predicted by the online websites Stabase (https://starbase.sysu.edu.cn) and Diana (https://diana.imis.athena-innovation.gr/Diana Tools/index.php?r=microT_CDS/), respectively. The wild-type (WT) circCYP51A1 or KLF12 3′-untranslated regions (3′UTR) fragments

included the binding sequence of miR-490-3p and circCYP51A1 or KLF12 mutant (MUT) binding sites were cloned into the pGL3 vector (Promega Corporation), namely circCYP51A1-WT, circCYP51A1-MUT, KLF12 3′ UTR-WT and KLF12 3′ UTR -MUT. Corresponding reporter vectors and miR-490-3p mimic or miR-NC were co-transfected in U2OS and MG63 cells by using Lipofectamine 3000 (Thermo Fisher) for 48 h. Subsequently, the relative luciferase activity was measured by the dual-luciferase reporter assay system (Promega, Madison, WI, USA).

2.11. Xenograft mice model

To establish the xenograft tumor model, the sh-NC or sh-circCYP51A1 was transfected in MG63 or MNNG/HOS cells. 10 male BALB/c nude mice (6 weeks old, n = 5 per group) were commercially acquired from Shanghai Experimental Animal Center (SLAC, Shanghai, China). All animal studies got the approval of the Research Ethics Committee of Cangzhou Central Hospital. Approximately 1×10^6 MG63 or MNNG/HOS cells stably expressing sh-NC or sh-circCYP51A1 were subcutaneously implanted into the mice. Tumor volume was monitored and calculated once a week for 28 days. Ultimately, all research mice were sacrificed and the tumor tissues were removed for further analysis.
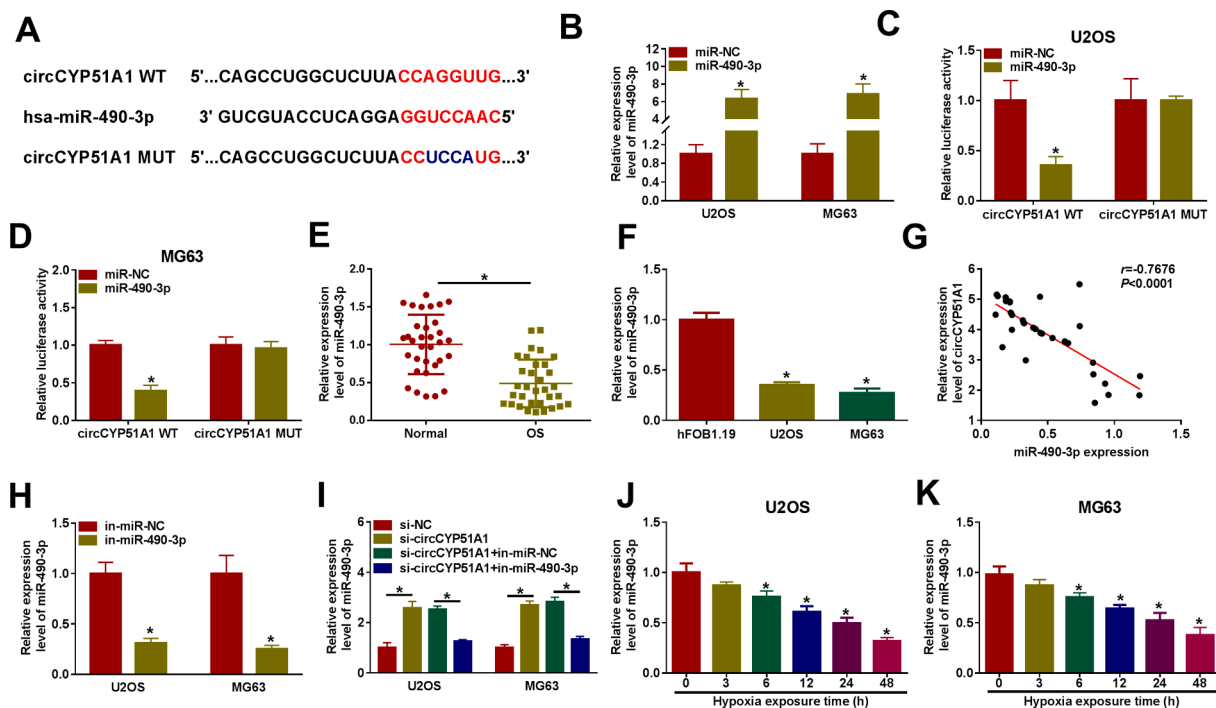
Fig. 3. CircCYP51A1 acted as a sponge of miR-490-3p in OS cells. (A) The binding sites between miR-490-3p and circCYP51A1 were predicted by starbase. (B) The overexpression efficiency of miR-490-3p was detected by qRT-PCR in U2OS and MG63 cells. (C-D) The binding relationship between circCYP51A1 and miR-490-3p was verified by dual-luciferase reporter assay in U2OS and MG63 cells. (E-F) The expression of miR-490-3p in OS tissues and cells was tested by qRT-PCR. (G) Correlation analysis of circCYP51A1 and miR-490-3p expression in OS tissues. (H) The knockdown efficiency of miR-490-3p inhibitor was detected by qRT-PCR. (I) miR-490-3p expression was checked by qRT-PCR in U2OS and MG63 cells transfected with si-NC, si-circCYP51A1, si-circCYP51A1 + in-miR-NC, or si-circCYP51A1 + in-miR-490-3p. (J-K) Relative expression of miR-490-3p in U2OS and MG63 cells exposed to hypoxia treatment for 0, 3, 6, 12, 24, or 48 h was detected by qRT-PCR. *$P < 0.05$.

2.12. Immunohistochemistry assay

Paraffin-embedded specimens were sectioned and heated at 60 °C, followed by rehydrated through alcohol. Antigen retrieval was performed in a microwave oven. Subsequently, endogenous peroxidase activity was performed using H_2O_2 and the sections were incubated with the antibodies against KLF12 (1:200; PA5-120729), GLUT1 (1:500; ab115730), HK2 (1:500; MA5-15679), LDHA (1:2000, ab52488) and MMP9 (1:500; MA5-15886). Immunoreactivity was visualized with DAB substrate. Finally, images were captured under a confocal microscope.

2.13. Statistical analysis

The results in our study were presented as mean ± standard deviation and data were obtained from 3 independent and not replicate experiments. All statistical analyses were executed by GraphPad Prism 7.0. The comparisons between two groups were assessed using Student's t test. One-way or two-way analysis of variance was used to comparison among three or more group results. *$P < 0.05$ was deemed as statistically significant difference.

3. Results

3.1. The expression level of circCYP51A1 was upregulated in OS cells under hypoxia

Firstly, the expression level of circCYP51A1 was analyzed using qRT-PCR in OS tissues and cells. As indicated in Fig. 1A, circCYP51A1 was drastically overexpressed in OS tissues (n = 33) when compared to the corresponding neighboring normal tissues (n = 33). In parallel, the level of circCYP51A1 was markedly increased in OS cells (U2OS and MG63) in comparison with human fetal osteoblastic cell line (hFOB1.19) (Fig. 1B).

Moreover, the expression of circCYP51A1 had no notable difference, while GAPDH RNA (linear RNA) expression was digested following RNase R treatment in U2OS and MG63 cells (Fig. 1C-D). In addition, the expression level of circCYP51A1 was determined in U2OS and MG63 cells after exposure in the hypoxia treatment (hypoxia chamber with 1 % O_2) in a time-dependent manner (0 h, 3 h, 6 h, 12 h, 24 h and 48 h). The result showed that the level of circCYP51A1 was up-regulated in U2OS and MG63 cells under hypoxia (Fig. 1E-F). These results indicated that circCYP51A1 level was notably enhanced in OS tissues and cells and was related to hypoxia.

3.2. CircCYP51A depletion suppressed hypoxia-induced cell proliferation, migration, invasion and glycolysis in OS cells

The subcellular localization of circCYP51A1 was detected in OS cells by using nuclear and cytoplasmic fraction assay. As shown in Fig. 2A, circCYP51A1 was mainly distributed in the cytoplasm of U2OS and MG63 cells. QRT-PCR was used to analyze the transfection efficiency of circCYP51A1. After hypoxia treatment, the expression of circCYP51A1 was remarkably increased in U2OS and MG63 cells when compared with normoxic treatment, while this effect was reversed by the knockdown of circCYP51A1 (Fig. 2B). Moreover, the colony formation assay illustrated that hypoxia treatment raised the proliferation of U2OS and MG63 cells, whereas these effects were weakened by circCYP51A1 silencing (Fig. 2C). Transwell and wound healing assays uncovered that circCYP51A1 knockdown reversed hypoxia-induced promotion effects on the migration and invasion of U2OS and MG63 cells (Fig. 2D-F). Meanwhile, the lactate production and glucose consumption were markedly induced after 48 h of hypoxia treatment, which was abated by silencing of circCYP51A1 (Fig. 2G-H). Simultaneously, glycolysis-associated marker (GLUT1, HK2 and LDHA) expression levels were assessed in U2OS and MG63 cells by Western blot. GLUT1, HK2 and
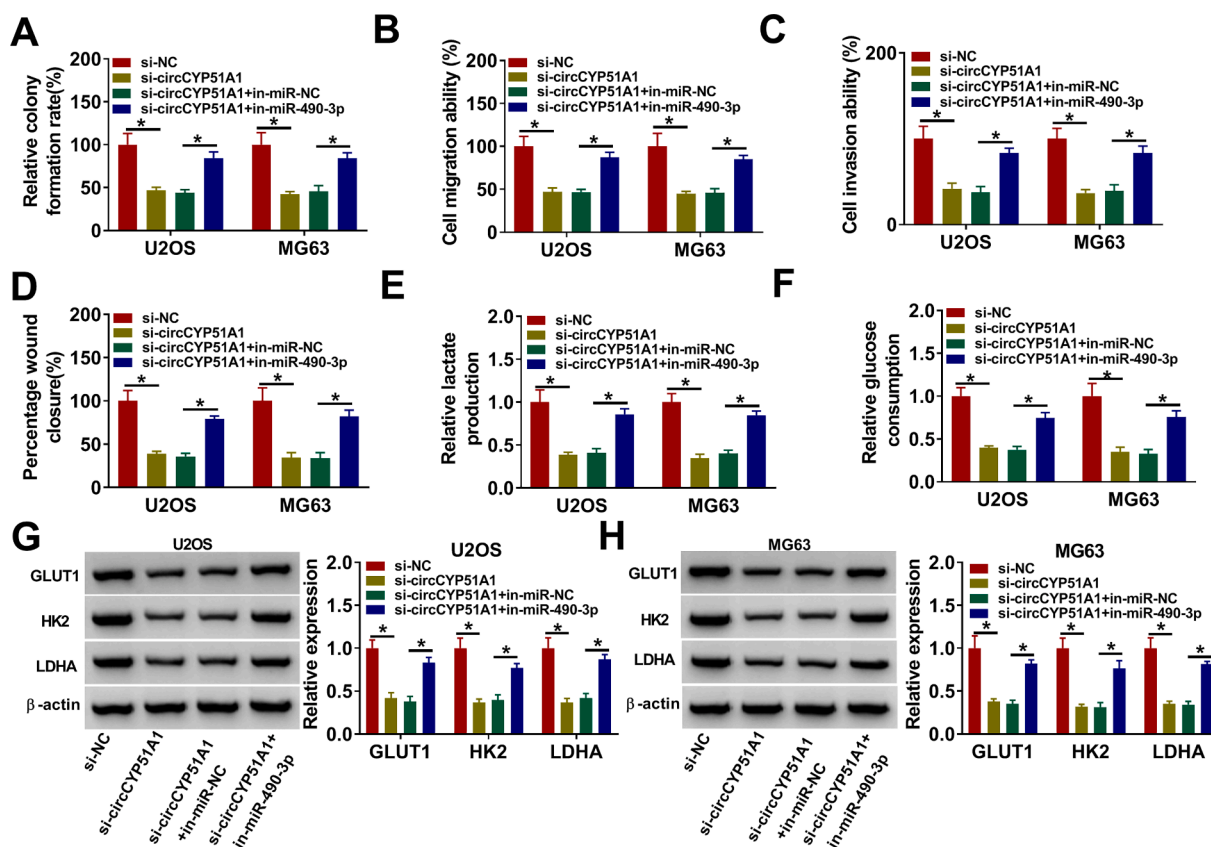
Fig. 4. Silencing of circCYP51A1 impaired the proliferation, migration, invasion and glycolysis of OS cells under hypoxia by targeting miR-490-3p. (A-H) U2OS and MG63 cells were transfected with si-NC, si-circCYP51A1, si-circCYP51A1 + in-miR-NC, or si-circCYP51A1 + in-miR-490-3p after treatment of hypoxia. (A) Cell proliferative capacity was evaluated by colony formation assay. (B-D) Cell migration and invasion were measured by using transwell assays or wound healing assay. (E-F) Lactate production and glucose consumption levels in U2OS and MG63 cells were detected using lactate and glucose assay kits, respectively. (G-H) The protein levels of GLUT1, HK2 and LDHA were examined by western blot. *$P < 0.05$.

LDHA expression levels were remarkably boosted in U2OS and MG63 cells following hypoxia stimulation, which was offset by treatment of si-circCYP51A1 (Fig. 2I-J). Further, we observed that circCYP51A1 knockdown repressed U2OS and MG63 cell colony formation ability, migration, invasion, lactate production and glucose consumption under normoxia (Figure S1). All these outcomes supported that the absence of circCYP51A1 suppressed hypoxia-induced OS cell proliferation, migration, invasion and glycolysis.

3.3. CircCYP51A1 functioned as a molecular sponge of miR-490-3p in OS cells

Starbase (http://starbase.sysu.edu.cn), one of the online bioinformatics tools, was used to predict the target miRNAs of circCYP51A1. This database displayed the complementary binding sites between circCYP51A1 and miR-490-3p (Fig. 3A). The expression level of miR-490-3p was notably elevated in U2OS and MG63 cells transfected with miR-490-3p mimic (Fig. 3B). Subsequently, dual-luciferase reporter assay was used to examine the relationship between circCYP51A1 and miR-490-3p in U2OS and MG63 cells. The results manifested that overexpression of miR-490-3p greatly decreased the luciferase activity of circCYP51A1 WT group in U2OS and MG63 cells, whereas it did not affect the luciferase activity of circCYP51A1 MUT group (Fig. 3C-D). In addition, qRT-PCR results reflected that the level of miR-490-3p was declined in OS tissues and cells in contrast with the neighboring normal tissues and hFOB1.19 cells (Fig. 3E-F). Besides, a negative correlation between circCYP51A1 and miR-490-3p expression was found in OS tissues (Fig. 3G). As indicated in Fig. 3H, the miR-490-3p level was suppressed by transfection of miR-490-3p inhibitor in U2OS and MG63

cells. Moreover, miR-490-3p level was increased in U2OS and MG63 cells with knockdown of circCYP51A1, while this effect could was eliminated by co-transfection of in-miR-490-3p (Fig. 3I). After 48 h of hypoxia treatment, the expression level of miR-490-3p was reduced in U2OS and MG63 cells in a time-dependent manner (Fig. 3J-K). Taken together, these findings suggested that circCYP51A1 acted as a miR-490-3p sponge to competitively modulate miR-490-3p activity.

3.4. Silencing of circCYP51A impeded cell proliferation, migration, invasion and glycolysis under hypoxia via targeting miR-490-3p in OS cells

To explore whether circCYP51A1 combined with miR-490-3p to mediate the progression of OS cells under hypoxic treatment, U2OS and MG63 cells were transfected with si-NC, si-circCYP51A1, si-circCYP51A1 + in-miR-NC and si-circCYP51A1 + in-miR-490-3p. Colony formation, transwell and wound healing assays were used to measure cell proliferation, migration and invasion, respectively. This data explained that in-miR-490-3p could partly eliminate the inhibitory effect of circCYP51A1 on cell proliferation (Fig. 4A), migration (Fig. 4B, D) and invasion (Fig. 4C) under hypoxia condition in U2OS and MG63 cells. Moreover, miR-490-3p deficiency could ameliorate the inhibitory effect of circCYP51A1 inhibition on lactate production (Fig. 4E) and glucose consumption (Fig. 4F) in U2OS and MG63 cells under hypoxia condition. Simultaneously, glycolysis-associated proteins (GLUT1, HK2 and LDHA) were determined, and the results that miR-490-3p down-regulation could block the inhibitory effect of circCYP51A1 knockdown on GLTU1, HK2 and LDHA protein levels in U2OS and MG63 cells under hypoxia condition (Fig. 4G-H). These findings speculated that knock-down of circCYP51A1 inhibited the proliferation, migration, invasion
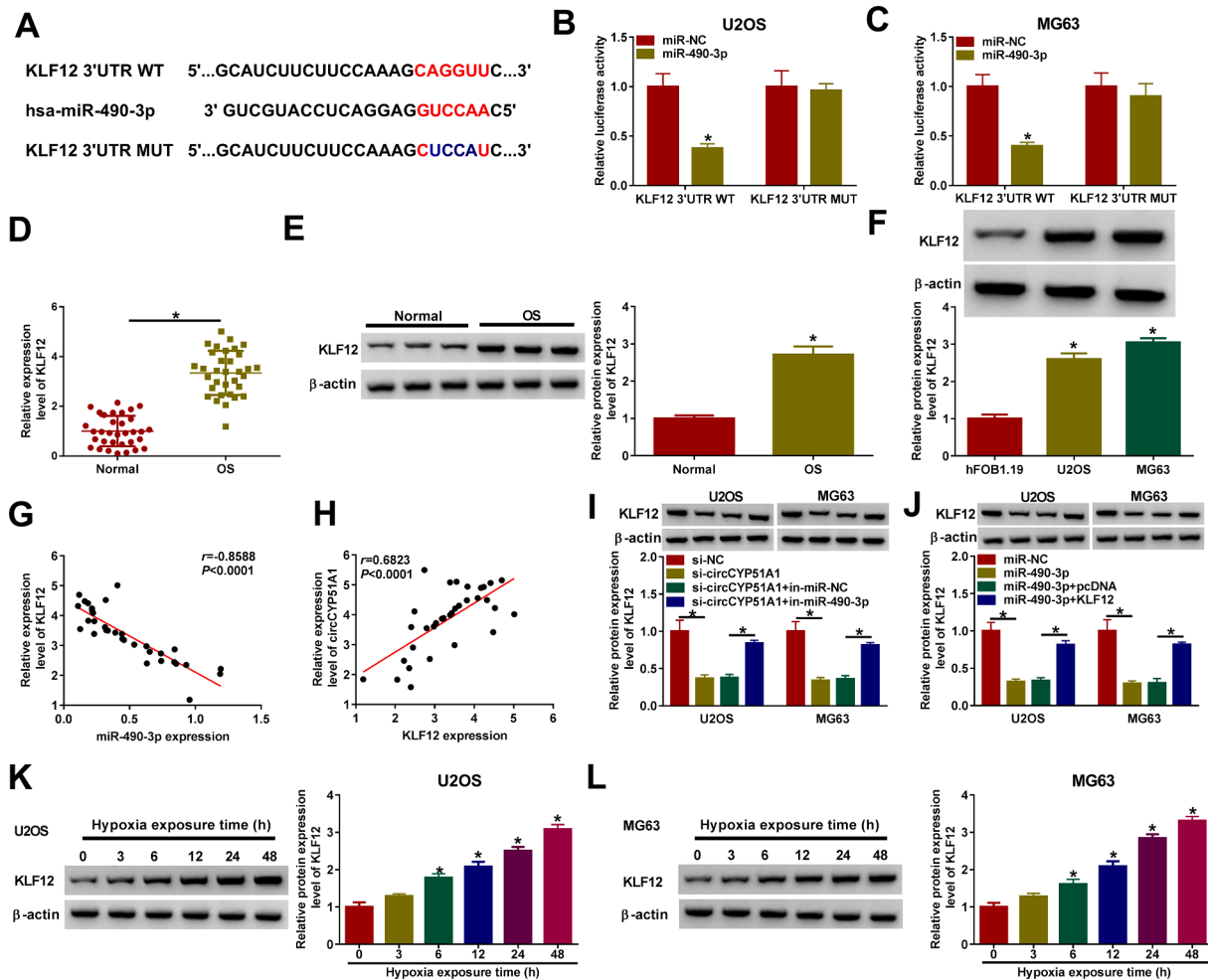
Fig. 5. circCYP51A1 mediated KLF12 expression by associating with miR-490-3p. (A) KLF12 was predicted to be the target of miR-490-3p via DIANA. (B-C) Luciferase reporter assay was performed to validate the interaction between miR-490-3p and KLF12. (D-E) The mRNA and protein levels of KLF12 were examined in OS tissues and normal tissues. (F) The expression of KLF12 in hFOB1.19, U2OS and MG63 cells was determined by western blot. (G) Correlation analysis of miR-490-3p and KLF12 expression in OS tissues. (H) Correlation analysis of circCYP51A1 and KLF12 expression in OS tissues. (I) The protein level of KLF12 was examined in U2OS and MG63 cells transfected with si-NC, si-circCYP51A1, si-circCYP51A1 + in-miR-NC, or si-circCYP51A1 + in-miR-490-3p. (J) KLF12 protein level was performed in U2OS and MG63 cells transfected with miR-NC, miR-490-3p, miR-490-3p + pcDNA or miR-490-3p + KLF12. (K-L) Relative expression of miR-490-3p in U2OS and MG63 cells after hypoxia exposure was detected by western blot. *$P < 0.05$.

and glycolysis of OS cells under hypoxia condition by sponging miR-490-3p.

3.5. CircCYP51A1 could regulate the expression of KLF12 by sponging miR-490-3p

The 3′UTR of KLF12 was found to possess a complementary binding site for miR-490-3p (Fig. 5A). Next, the dual luciferase reporter assay verified that miR-490-3p overexpression reduced the luciferase activity of KLF12 3′UTR WT, but the relative luciferase activity of KLF12 3′UTR MUT group was not affected in U2OS and MG63 cells (Fig. 5B-C). Moreover, qRT-PCR and western blot assay results exhibited that KLF12 mRNA and protein levels in OS tissues and cells were strikingly enhanced (Fig. 5D-F). In addition, the expression level of KLF12 mRNA was inversely associated with miR-490-3p expression (Fig. 5G), while KLF12 expression level was positively correlated with circCYP51A1 abundance in OS tissues (Fig. 5H). Deficiency of circCYP51A1 inhibited KLF12 expression level, while miR-490-3p inhibition abated the effect (Fig. 5I). Overexpression of miR-490-3p also inhibited KLF12 protein level, but the level of KLF12 was significantly elevated following the co-transfection of KLF12 (Fig. 5J). Besides, the protein levels of KLF12 were progressively exalted in U2OS and MG63 cells after stimulation of

hypoxia treatment with time (Fig. 5K-L). Collectively, all these data displayed that circCYP51A1 regulated KLF12 expression by sponging miR-490-3p.

3.6. Overexpression of KLF12 abolished the effects of miR-490-3p overexpression on OS cell proliferation, migration, invasion and glycolysis under hypoxia condition

Colony formation, transwell and wound healing assays revealed that overexpression of miR-490-3p inhibited OS cell proliferation (Fig. 6A), migration (Fig. 6B, D) and invasion (Fig. 6C) under hypoxia in U2OS and MG63 cells, while these effects were abrogated by the overexpression of KLF12. In addition, overexpression of miR-490-3p restrained lactate production (Fig. 6E), glucose consumption (Fig. 6F) and glycolysis-associated proteins (GLUT1, HK2 and LDHA) (Fig. 6G-H) in U2OS and MG63 cells under hypoxia, whereas these effects were eliminated by KLF12 overexpression. In addition, KLF12 knockdown repressed U2OS and MG63 cell colony formation ability, migration, invasion, lactate production and glucose consumption (Figure S2). In summary, these outcomes indicated miR-490-3p affected the proliferation, migration, invasion and glycolysis of OS cells under hypoxia by functional targeting KLF12.
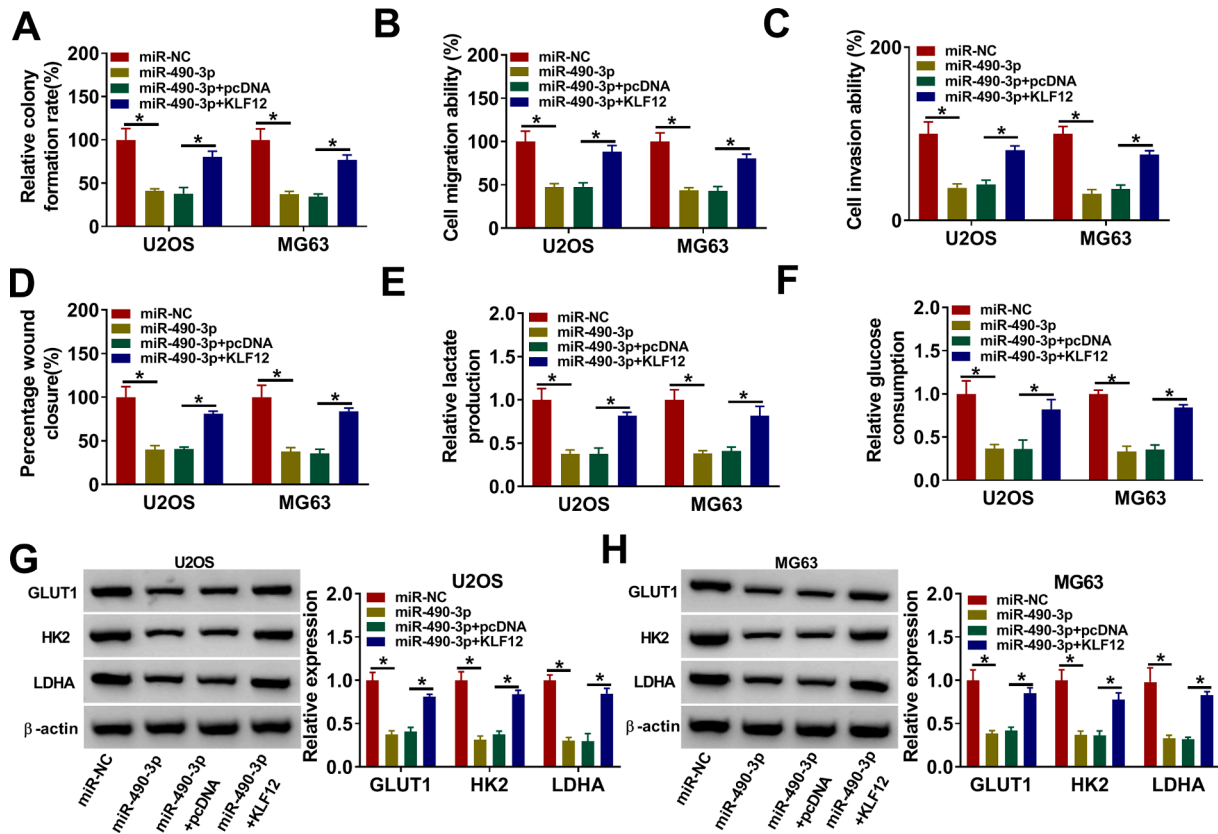
Fig. 6. KLF12 overexpression reversed the effect of miR-490-3p overexpression on OS progression under hypoxia. (A-H) U2OS and MG63 cells were transfected with miR-NC, miR-490-3p, miR-490-3p + pcDNA or miR-490-3p + KLF12 after treatment of hypoxia. (A) Cell proliferative capacity was evaluated by colony formation assay. (B-D) Cell migration and invasion were measured by using transwell assays or wound healing assay. (E-F) Lactate production and glucose consumption levels in U2OS and MG63 cells were detected using lactate and glucose assay kits, respectively. (G-H) The protein levels of GLUT1, HK2 and LDHA levels were examined by western blot. *$P < 0.05$.

3.7. CircCYP51A1 depletion suppressed OS xenograft tumor growth

In vivo, xenograft mice models were established to further explore the function of circCYP51A1. The results displayed that tumor volume (Fig. 7A and Fig. S3A) and weight (Fig. 7B and Fig. S3B) were markedly decreased in sh-circCYP51A1 group in comparison to the sh-NC group. In addition, we found that circCYP51A1 knockdown significantly reduced the number of metastatic nodes in the lung (Fig. S3C). Notably, the expression level of circCYP51 and KLF12 were reduced, while miR-490-3p expression level was significantly increased in the sh-circCYP51A1 group in comparison to sh-NC group (Fig. 7C-E and Fig. S3D). Further, we observed that the positive expression rates of KLF12, GLUT1, HK2, LDHA and MMP9 were lower in the sh-circCYP51A1 group than in the sh-NC group (Fig. 7F). To sum up, these data indicated that the knockdown of circCYP51A1 hindered tumor growth *in vivo* by regulating miR-490-3p/KLF12 axis.

4. Discussion

OS is defined by the presence of malignant mesenchymal cells producing osteoid samples and immature bone [27]. It is a highly invasive tumor with high mortality in children and adolescent patients [28]. Hypoxia is a key characteristic of human cancer and plays an important role in metastasis, apoptosis, drug resistance and glycolytic metabolism [29–31]. Many data have found that circRNAs are involved in the regulation of tumor progress under hypoxia, but few studies have been carried out in OS. In the present study, circCYP51A1 was overexpressed in hypoxia-induced OS cells. Silencing of circCYP51A1 suppressed hypoxia-induced cell proliferation, migration, invasion and glycolysis

by regulating miR-490-3p/KLF12 axis.

CircRNAs work as oncogenes or suppressor genes to regulate the biological function of human cancer [32]. For instance, up-regulation of circ_0004018 inhibited HCC cell proliferation and metastasis by sponging miR-1197/PTEN axis [33]. Deficiency of circDNA2 down-regulated CCDC6 level and suppressed the proliferative capacities of GC cells by sponging miR-149-5p [34]. Hsa_circ_0081001 (circ-CYP51A1) is found as an oncogenic factor in OS [35]. Another study reported that circ_0081001 contributed to methotrexate sensitivity through the regulation of miR-494-3p/transglutaminase 2 pathway [36]. In this current study, the level of circCYP51A1 was significantly elevated, which was consistent with the previous reports [14]. In addition, our data was the first to show that circCYP51A1 knockdown blocked OS cells proliferation, migration, invasion and glycolytic metabolism under hypoxia treatment.

CircRNA regulates mRNA expression to exert its biological functions in various cancers by sponging miRNA, which is well known. Herein, the relationship between the circCYP51A1 and miR-490-3p was predicted by starbase online website. Our work found that circCYP51A1 and miR-490-3p have complementary binding sites. As a tumor suppressor, miR-490-3p has been reported to participate in the occurrence and development of human diseases in previous research. For instance, miR-490-3p expression level was down-regulated and overexpression of miR-490-3p inhibited the biological progression of CRC [37]. Similarly, miR-490-3p was related to the biological progress in OS. Previous studies have shown that miR-490-3p downregulation is significantly associated with distant metastasis and relapse-free survival of OS [38]. MiR-490-3p restrained cell proliferation and metastasis and boosted cell apoptosis by OS [39,40]. In the current work, miR-490-3p was notably reduced in
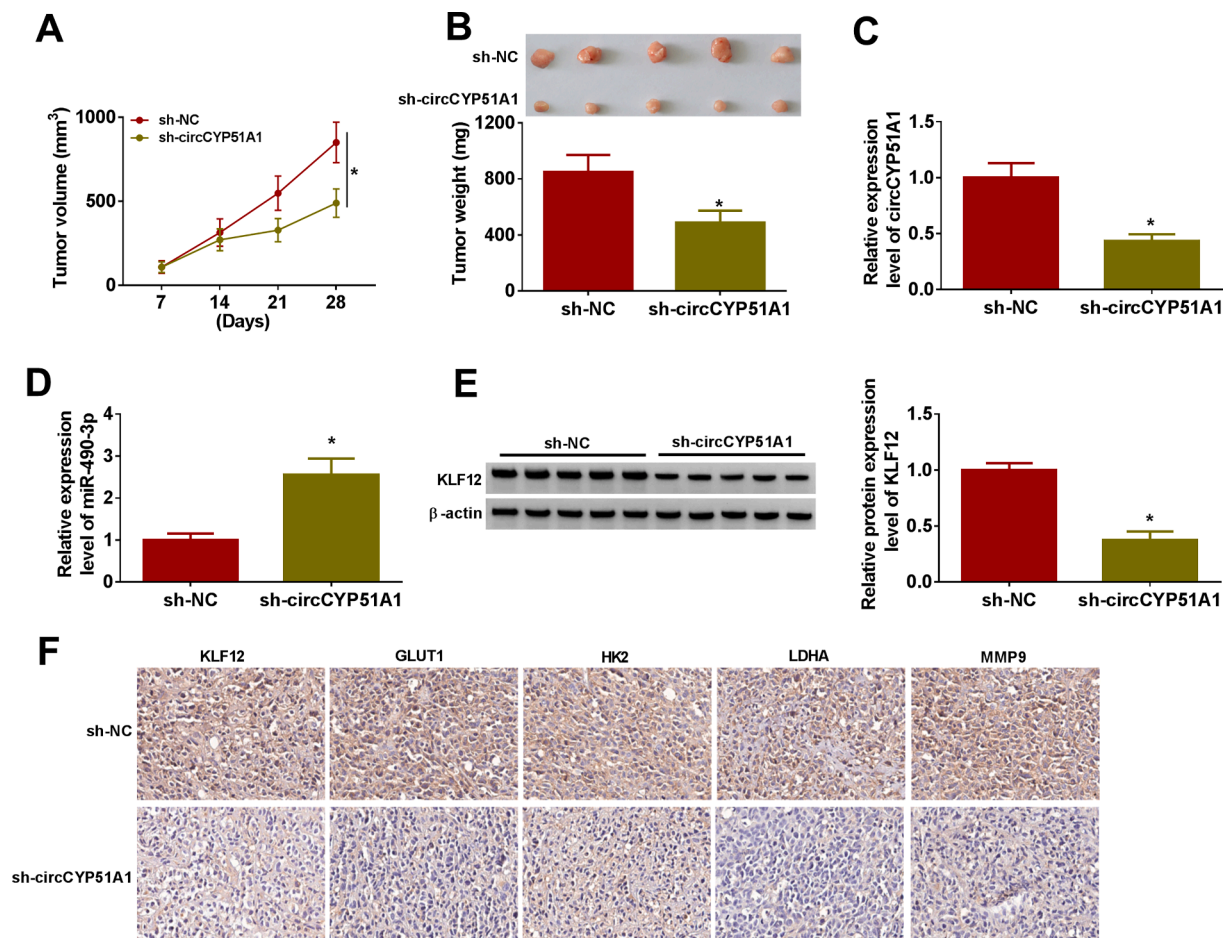
Fig. 7. Depletion of circCYP51A1 hindered OS tumor growth *in vivo*. MG63 cells stable expressing sh-NC or sh-circCYP51A1 were subcutaneously injected into nude mice (n = 5 in each group). (A) Tumor volumes were measured every week for four weeks. (B) Tumor size was measured after 28 days. (C-E) The levels of circCYP51A1, miR-490-3p and KLF12 were measured by qRT-PCR or western blot. (F) The positive expression rates of KLF12, GLUT1, HK2, LDHA and MMP9 in tumor tissues were analyzed by IHC assay. *$P < 0.05$.

OS cells under hypoxia condition, and miR-490-3p downregulation reversed the inhibitory effect of circCYP51A1 silencing on OS progression under hypoxia condition.

KLF12 has constantly been detected in the progression of tumors. For instance, KLF12 was up-regulated and could eliminate the inhibitory effect of miR-138-5p in GC cells [41]. Overexpression of KLF12 promoted the metastasis and drug resistance of BC cells [42]. This study demonstrated for the first time that KFL12 was the target gene for miR-490-3p, which was predicted by Diana website. Our work found that KLF12 was overexpressed in OS cells, which was similar to the previous research. Besides, the expression level of KLF12 was strikingly increased in OS with hypoxia treatment. Overexpression of KLF12 weakened miR-490-3p-induced cell progression in OS cells under hypoxia condition. Moreover, knockdown of circCYP51A1 suppressed tumor growth by increasing miR-490-3p and reducing KLF12 *in vivo*.

In conclusion, the present studies manifested that the deficiency of circCYP51A1 inhibited cell proliferation, migration, invasion and glycolysis by sponging miR-490-3p and regulating KLF12 in OS cells under hypoxia treatment. The current studies revealed that circCYP51A1-miR-490-3p-KLF12 network provided a novel strategy for understanding the progression of OS under hypoxia condition.

Funding

Declaration of Competing Interest

The authors declare that they have no known competing financial interests or personal relationships that could have appeared to influence the work reported in this paper.

Acknowledgement

Appendix A. Supplementary data

Supplementary data to this article can be found online at https://doi.org/10.1016/j.jbo.2022.100455.

References

[1] R. Zhu, X. Li, Y. Ma, miR-23b-3p suppressing PGC1alpha promotes proliferation through reprogramming metabolism in osteosarcoma, Cell Death Dis. 10 (6) (2019) 381.
[2] Y. Shen, J. Xu, J. Pan, Y. Zhang, Y. Weng, D. Zhou, S. He, LncRNA KCNQ1OT1 sponges miR-34c-5p to promote osteosarcoma growth via ALDOA enhanced aerobic glycolysis, Cell Death Dis. 11 (4) (2020).
[3] J. Leng, et al., miR15a represses cancer cell migration and invasion under conditions of hypoxia by targeting and downregulating Bcl2 expression in human osteosarcoma cells, Int. J. Oncol. 52 (4) (2018) 1095–1104.
[4] Q. Du, J. Han, S. Gao, S. Zhang, Y. Pan, Hypoxia-induced circular RNA hsa_circ_0008450 accelerates hepatocellular cancer progression via the miR-431/AKAP1 axis, Oncol. Lett. 20 (6) (2020).

[5] R. Huang, X. Zong, Aberrant cancer metabolism in epithelial-mesenchymal transition and cancer metastasis: Mechanisms in cancer progression, Crit. Rev. Oncol. Hematol. 115 (2017) 13–22.

[6] S. Ren, J. Liu, Y. Feng, Z. Li, L. He, L. Li, X. Cao, Z. Wang, Y. Zhang, Knockdown of circDENND4C inhibits glycolysis, migration and invasion by up-regulating miR-200b/c in breast cancer under hypoxia, J. Exp. Clin. Cancer Res. 38 (1) (2019).

[7] C. Du, et al., Hypoxia-inducible MiR-182 promotes angiogenesis by targeting RASA1 in hepatocellular carcinoma, J. Exp. Clin. Cancer Res. 34 (2015) 67.

[8] S. Chaichian, R. Shafabakhsh, S.M. Mirhashemi, B. Moazzami, Z. Asemi, Circular RNAs: A novel biomarker for cervical cancer, J. Cell. Physiol. 235 (2) (2020) 718–724.

[9] L.S. Kristensen, T.B. Hansen, M.T. Venø, J. Kjems, Circular RNAs in cancer: opportunities and challenges in the field, Oncogene 37 (5) (2018) 555–565.

[10] D. Dou, et al., CircUBE2D2 (hsa_circ_0005728) promotes cell proliferation, metastasis and chemoresistance in triple-negative breast cancer by regulating miR-512-3p/CDCA3 axis, Cancer Cell Int. 20 (2020) 454.

[11] T. Wu, Y. Sun, Z. Sun, S. Li, W. Wang, B. Yu, G. Wang, Hsa_circ_0042823 accelerates cancer progression via miR-877-5p/FOXM1 axis in laryngeal squamous cell carcinoma, Ann. Med. 53 (1) (2021) 961–971.

[12] Fang, X., et al., Silencing circSLAMF6 represses cell glycolysis, migration, and invasion by regulating the miR-204-5p/MYH9 axis in gastric cancer under hypoxia. Biosci Rep, 2020. **40**(6).

[13] Z. Qiu, L. Wang, H. Liu, Hsa_circ_0001982 promotes the progression of breast cancer through miR-1287-5p/MUC19 axis under hypoxia, World J. Surg. Oncol. 19 (1) (2021) 161.

[14] Z. Kun-Peng, Z. Chun-Lin, H.u. Jian-Ping, Z. Lei, A novel circulating hsa_circ_0081001 act as a potential biomarker for diagnosis and prognosis of osteosarcoma, Int. J. Biol. Sci. 14 (11) (2018) 1513–1520.

[15] A.C. Panda, Circular RNAs Act as miRNA Sponges, Adv. Exp. Med. Biol. 1087 (2018) 67–79.

[16] B. Zhang, Z. Liu, J. Liu, K. Cao, W. Shan, Q. Wen, R. Wang, Long non-coding RNA ST8SIA6-AS1 promotes the migration and invasion of hypoxia-treated hepatocellular carcinoma cells through the miR-338/MEPCE axis, Oncol. Rep. 45 (1) (2021) 73–82.

[17] C. Zhao, X. Bai, X. Hu, Knockdown of lncRNA XIST inhibits hypoxia-induced glycolysis, migration and invasion through regulating miR-381-3p/NEK5 axis in nasopharyngeal carcinoma, Eur. Rev. Med. Pharmacol. Sci. 24 (5) (2020) 2505–2517.

[18] G.A. Calin, C.M. Croce, MicroRNA signatures in human cancers, Nat. Rev. Cancer 6 (11) (2006) 857–866.

[19] X. Cai, Y. Dai, P. Gao, G. Ren, D. Cheng, B.o. Wang, Y.i. Wang, J. Yu, Y. Du, X. Wang, B. Xue, LncRNA CCAT1 promotes prostate cancer cells proliferation, migration, and invasion through regulation of miR-490-3p/FRAT1 axis, Aging (Albany NY) 13 (14) (2021) 18527–18544.

[20] L. Zhang, B. Chi, J. Chai, L.i. Qin, G. Zhang, P. Hua, C. Jin, LncRNA CCDC144NL-AS1 Serves as a Prognosis Biomarker for Non-small Cell Lung Cancer and Promotes Cellular Function by Targeting miR-490-3p, Mol. Biotechnol. 63 (10) (2021) 933–940.

[21] Y. Chen, R. Zhang, Long non-coding RNA AL139002.1 promotes gastric cancer development by sponging microRNA-490-3p to regulate Hepatitis A Virus Cellular Receptor 1 expression, Bioengineered 12 (1) (2021) 1927–1938.

[22] Z. Mi, Y. Dong, Z. Wang, P. Ye, Biomarker potential of lncRNA GNAS-AS1 in osteosarcoma prognosis and effect on cellular function, J. Orthopaedic Surg. Res. 16 (1) (2021).

[23] J. Wang, J. Pu, Y. Zhang, T. Yao, Z. Luo, W. Li, G. Xu, J. Liu, W. Wei, Y. Deng, DANCR contributed to hepatocellular carcinoma malignancy via sponging miR-216a-5p and modulating KLF12, J. Cell. Physiol. 234 (6) (2019) 9408–9416.

[24] P. Song, S. Yin, Long non-coding RNA 319 facilitates nasopharyngeal carcinoma carcinogenesis through regulation of miR-1207-5p/KLF12 axis, Gene 680 (2019) 51–58.

[25] G. Wu, A. Zhang, Y. Yang, D. Wu, Circ-RNF111 aggravates the malignancy of gastric cancer through miR-876-3p-dependent regulation of KLF12, World J. Surg. Oncol. 19 (1) (2021).

[26] J. Yuan, J. Kang, M. Yang, Long non-coding RNA ELF3-antisense RNA 1 promotes osteosarcoma cell proliferation by upregulating Kruppel-like factor 12 potentially via methylation of the microRNA-205 gene, Oncol. Lett. 19 (3) (2020) 2475–2480.

[27] Z. Shi, Y.e. Wen, S. Zhang, X. Cheng, Circular RNA MTO1 intercorrelates with microRNA-630, both associate with Enneking stage and/or pathological fracture as well as prognosis in osteosarcoma patients, J. Clin. Lab. Anal. 35 (11) (2021) e23987.

[28] Y. Gao, C. Liu, X. Zhao, C. Liu, W. Bi, J. Jia, hsa_circ_0000006 induces tumorigenesis through miR-361-3p targeting immunoglobulin-like domains protein 1 (LRIG1) in osteosarcoma, Ann. Transl. Med. 9 (15) (2021).

[29] X. Li, C. Zhang, Y. Tian, Long non-coding RNA TDRG1 promotes hypoxia-induced glycolysis by targeting the miR-214-5p/SEMA4C axis in cervical cancer cells, J. Mol. Histol. 52 (2) (2021) 245–256.

[30] D. Wu, B. Chen, F. Cui, X. He, W. Wang, M. Wang, Hypoxia-induced microRNA-301b regulates apoptosis by targeting Bim in lung cancer, Cell Prolif. 49 (4) (2016) 476–483.

[31] L. Yu, J. Li, B. Peng, P. Cai, B. Zhao, Y. Chen, H. Zhu, CircASXL1 Knockdown Restrains Hypoxia-Induced DDP Resistance and NSCLC Progression by Sponging miR-206, Cancer Manage. Res. 13 (2021) 5077–5089.

[32] W.W. Du, W. Yang, E. Liu, Z. Yang, P. Dhaliwal, B.B. Yang, Foxo3 circular RNA retards cell cycle progression via forming ternary complexes with p21 and CDK2, Nucl. Acids Res. 44 (6) (2016) 2846–2858.

[33] H.e. Wang, Q. Zhang, W. Cui, W. Li, J. Zhang, Circ_0004018 suppresses cell proliferation and migration in hepatocellular carcinoma via miR-1197/PTEN/PI3K/AKT signaling pathway, Cell Cycle (Georgetown, Tex.) 20 (20) (2021) 2125–2136.

[34] D. Jin, et al., CCDC6Circular RNA circDNA2 upregulates expression to promote the progression of gastric cancer via miR-149-5p suppression, Mol. Ther. Nucl. Acids 26 (2021) 360–373.

[35] S. Liu, K. Duan, X. Zhang, X. Cao, X. Wang, F. Meng, H. Liu, B. Xu, X.i. Wang, Circ_0081001 down-regulates miR-494-3p to enhance BACH1 expression and promotes osteosarcoma progression, Aging 13 (13) (2021) 17274–17284.

[36] W. Wei, L. Ji, W. Duan, J. Zhu, Circular RNA circ_0081001 knockdown enhances methotrexate sensitivity in osteosarcoma cells by regulating miR-494-3p/TGM2 axis, J Orthop. Surg. Res. 16 (1) (2021).

[37] X. Liu, B. He, T. Xu, Y. Pan, X. Hu, X. Chen, S. Wang, MiR-490-3p Functions As a Tumor Suppressor by Inhibiting Oncogene VDAC1 Expression in Colorectal Cancer, J. Cancer 9 (7) (2018) 1218–1230.

[38] B. Tang, et al., Decreased expression of miR-490-3p in osteosarcoma and its clinical significance, Eur. Rev. Med. Pharmacol. Sci. 21 (2) (2017) 246–251.

[39] J. He, J. Guan, S. Liao, Z. Wu, B. Liu, H. Mo, Z. Yuan, Long Noncoding RNA CCDC144NL-AS1 Promotes the Oncogenicity of Osteosarcoma by Acting as a Molecular Sponge for microRNA-490-3p and Thereby Increasing HMGA2 Expression, OncoTargets Ther. 14 (2021) 1–13.

[40] Liu, W., et al., MicroRNA-490-3p regulates cell proliferation and apoptosis by targeting HMGA2 in osteosarcoma. FEBS Lett, 2015. **589**(20 Pt B): p. 3148-53.

[41] Y. Fan, et al., Depletion of Circular RNA circ_CORO1C Suppresses Gastric Cancer Development by Modulating miR-138-5p/KLF12 Axis, Cancer Manage. Res. 13 (2021) 3789–3801.

[42] D. Zhou, et al., Long non-coding RNA NEAT1 transported by extracellular vesicles contributes to breast cancer development by sponging microRNA-141-3p and regulating KLF12, Cell Biosci. 11 (1) (2021) 68.